Hybrid, experimental and computational, investigation of mechanical components

Cosme Furlong and **Ryszard J. Pryputniewicz**

Center for Holographic Studies and Laser μmechaTronics
Department of Mechanical Engineering
Worcester Polytechnic Institute
Worcester, Massachusetts 01609-2280

ABSTRACT

Computational and experimental methodologies have unique features for the analysis and solution of a wide variety of engineering problems. Computations provide results that depend on selection of input parameters such as geometry, material constants, and boundary conditions which, for correct modeling purposes, have to be appropriately chosen. In addition, it is relatively easy to modify the input parameters in order to computationally investigate different conditions. Experiments provide solutions which characterize the actual behavior of the object of interest subjected to specific operating conditions. However, it is impractical to experimentally perform parametric investigations. This paper discusses the use of a hybrid, computational and experimental, approach for study and optimization of mechanical components. Computational techniques are used for modeling the behavior of the object of interest while it is experimentally tested using noninvasive optical techniques. Comparisons are performed through a fringe predictor program used to facilitate the correlation between both techniques. In addition, experimentally obtained quantitative information, such as displacements and shape, can be applied in the computational model in order to improve this correlation. The result is a validated computational model that can be used for performing quantitative analyses and structural optimization. Practical application of the hybrid approach is illustrated with a representative example which demonstrates the viability of the approach as an engineering tool for structural analysis and optimization.

Keywords: hybrid methodologies, structural optimization, electro-optic holography, shape measurements, displacement measurements, fringe prediction.

1. INTRODUCTION

Computational methodologies have recently reached levels in which a mechanical component can be completely dimensioned and analyzed[1]. With these methodologies, parametric studies of the effects of different boundary conditions, loadings, and material properties can be investigated. In addition, structural optimization can be performed through a computationally intensive iterative procedure using methods such as the finite or boundary element combined with mathematical programming techniques[2]. Computational solutions depend on appropriate selection of modeling parameters, such as material constants, boundary conditions, and loads. Therefore, solutions may lack any significance if modeling parameters are not selected properly.

Experimental noninvasive optical measuring methodologies, such as electro-optic holography (EOH), are available for performing studies of mechanical components. EOH can provide qualitative information in real-time through interferograms and quantitative information can be obtained by processing the interferograms[3]. Quantitative information includes displacements and or deformations obtained after the object of interest has been subjected to specific boundary and loading conditions. In addition, it is possible to perform geometrical measurements of mechanical components using optical contouring. Results obtained with noninvasive optical techniques are valuable information since they are a measure of the behavior of the actual object of interest subjected to realistic operating conditions.

An effective study and structural optimization of mechanical components should include the use of both computational and experimental methodologies. Computational investigations permit parametric studies and determination of critical engineering design conditions while experimental investigations, especially those using optical techniques, provide quantitative information on the actual response of the structure of interest to the applied load conditions[4].

2. EXPERIMENTAL-COMPUTATION PROCEDURE

2.1. Computational investigations

Solutions of the partial differential equations (PDE) used for modeling different physical phenomena either cannot always be found using analytical considerations, or do not exist, or are limited to specific domains. For practical purposes, however, special techniques capable of solving these PDE have been developed for a wide range of different domains and boundary conditions. These techniques comprise the computational methodologies. Computational methodologies are computer-aided mathematical techniques for obtaining approximate numerical solutions to the PDE that predict the response of physical systems subjected to external influences[5]. Their applications extend to many areas that include solid mechanics, heat transfer, fluid mechanics, acoustics, and electromagnetism, as well as a coupled interaction of these phenomena[6]. Three computational methodologies have been used extensively for solving the PDE generated in many engineering and science fields. These include the finite differences (FD), finite element (FE), and boundary element (BE) methods. The fundamental principle of these methodologies is based on the reduction of governing PDE to an approximation in terms of algebraic equations. This reduction replaces continuous PDE, whose solution space is generally infinite dimensional, with a finite set of algebraic equations whose solution space is finite dimensional. In general, the reduction of continuous PDE into a set of discrete algebraic equations is performed by identifying a finite number of discrete points within the domain of interest. These points are called nodes and it is at these locations that approximations to the true solution are computed. For instance, consider the FE method in which the domain of interest is fully discretized into finite elements, Fig. 1. In the case of structural problems and a displacement formulation, the deformation field on each element is written in terms of known interpolating functions and unknown nodal displacements. By considering element e in the domain D of Fig. 1, coordinates (x,y) and displacements (u,v) within the element can be written, using two-dimensional isoparametric elements, as

$$x = \sum_{i=1}^{NN} N_i x_i \,, \quad y = \sum_{i=1}^{NN} N_i y_i \quad , \tag{1}$$

and

$$u = \sum_{i=1}^{NN} N_i u_i \,, \quad v = \sum_{i=1}^{NN} N_i v_i \quad , \tag{2}$$

where NN is the number of nodes in the element, (x_i,y_i) and (u_i,v_i) are the nodal coordinates and unknown nodal displacements, respectively, and N_i represents the interpolating or shape functions which for a linear approximation can be written as

$$N_i = \frac{1}{4}(1+\xi\xi_i)(1+\eta\eta_i) \quad , \tag{3}$$

with ξ and η being the natural coordinates $\in \{[-1,1],[-1,1]\}$ and ξ_i and η_i being the nodal coordinates in the unit parametric space. Therefore, the response of the entire domain is obtained by solving a system of equations that takes into consideration the effects of all the elements and has as unknowns the nodal, or discrete, displacements instead of a continuous displacement function.

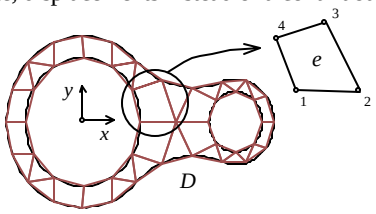

Fig. 1. Domain D discretized into finite elements, a simplified mesh is shown for clarity.

2.2. Experimental investigations: electro-optic holography (EOH)

EOH has been successfully applied to different fields of nondestructive testing of mechanical components subjected to static and dynamic loading conditions[3,4,7,8]. Being noninvasive and providing qualitative and quantitative full field information are some of the main advantages of EOH over other experimental techniques. In addition, it requires much less mechanical stability than that required in conventional holographic interferometry which makes it very suitable for on-site investigations. Electro-optic holography is based on a

combined use of speckle interferometry, phase stepping, and image acquisition and processing techniques. Figure 2 depicts a typical experimental setup for generation of interferograms using the EOH technique. In this system, the laser output is divided into two separate beams by means of a beam splitter BS. One of the beams is directed towards a beam expander BE to illuminate the object OB uniformly. This beam, modulated by interaction with an object is transmitted by the object imaging lens IL to the object input of the speckle interferometer SI. The other beam is directed toward a microscope objective MO and then to a single mode fiber optic probe that is connected to the reference input of SI. The object and reference beams are combined at the SI which is capable of projecting the combined signal onto the charge-coupled device (CCD) chip of the camera. The signal generated at the CCD camera, due to the interaction of object and reference beams, is directed to a pipeline image processor computer processing images at video rates. This computer is also controlling the phase shifter PS1 for introduction of phase steps between consecutive captured frames.

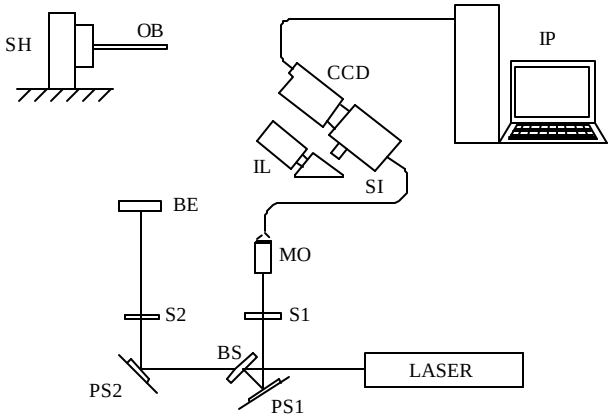

Fig. 2. Optical setup for recording and processing of electro-optic holograms: BS is the beam splitter, PS1 is the reference beam phase shifter, PS2 is the object beam phase shifter, S1and S2 are the reference and illumination beams shutters, MO is the microscope objective, SI is the speckle interferometer, IL is the object imaging lens, CCD is the imaging device, IP is the image processing computer, BE is the illumination beam expander, OB is the object under investigation, and SH is the PZT shaker for object excitation.

2.2.1. Static investigations

In EOH, information is extracted from the interference pattern of object and reference beams having complex light fields F_o and F_r. After the beam splitter, and considering phase stepping, irradiance of the combined wavefronts as recorded by the n-th video frame is described by

$$I_n = (F_o + F_r)(F_o + F_r)^*,$$
$$I_n = |A_o|^2 + |A_r|^2 + 2A_o A_r \cos\left[(\phi_o - \phi_r) + \Delta\theta_n\right], \quad (4)$$

where A_o and A_r are the amplitudes of the object and reference beams, ϕ_o is the randomly varying phase of the object beam, ϕ_r is the phase of the reference beam, and $\Delta\theta$ is the known phase step introduced between the frames[3,9]. To facilitate static investigations, the argument of the periodic term of Eq. 4 is modified to include the phase change due to static deformations of the object of interest subjected to specific loading and boundary conditions. This phase change is characterized by the fringe-locus function W, whose constant values define fringe loci on the surface of the object as

$$W(x,y) = 2\pi n(x,y) = \mathbf{K} \cdot \mathbf{L}, \quad (5)$$

where $n(x,y)$ is the interferometric fringe order at the (x,y) location in the image space, $\mathbf{K}$ is the sensitivity vector, and $\mathbf{L}$ the displacement vector. Therefore, the irradiance from a deformed object can be described as

$$I'_n = I_o + I_r + 2A_o A_r \cos(\Delta\phi + W + \Delta\theta_n), \quad (6)$$

where $\Delta f = f_o - f_r$, and I_o and I_r represent the intensities of the object and reference beams, respectively. In Eq. 6, I_o is assumed to remain constant and the (x,y) arguments were omitted for clarity. Since it is W which carries information pertaining to mechanical displacements, the EOH's video frame processing algorithm eliminates Δf from the argument of the periodic function of the irradiance distributions given in Eqs 4 and 6, yielding an image which has intensity modulated by a periodic function with W as the argument[3].

The EOH can work in display and data mode. In display mode, interference patterns are observed at video rate speed and are modulated by a cosinusoidal function of the form

$$8A_o A_r \cos\left(\frac{W}{2}\right) , \tag{7}$$

which is obtained by performing specific algebraic operations between frames acquired at the undeformed and deformed states, described by Eqs 4 and 6, respectively. This mode is used for adjusting the EOH system and for qualitative investigations. Data mode is used for performing quantitative investigations. In the data mode, two images are generated: a cosinusoidal image,

$$D = 64A_o^2 A_r^2 \cos(W) , \tag{8}$$

and a sinusoidal image,

$$N = 64A_o^2 A_r^2 \sin(W) , \tag{9}$$

which are processed simultaneously to produce quantitative results by computing[3,10]

$$W = \tan^{-1}\left(\frac{N}{D}\right) . \tag{10}$$

Figure 3a depicts a typical interferogram obtained with the EOH system functioning in static display mode.

2.2.2. Dynamic investigations

For performing dynamic investigations, or modal analysis, using the EOH, it is necessary to take into consideration a time varying fringe-locus function W_t which is related to periodic motion of the object under investigation[3,4]. Using Eq. 6, it is possible to write

$$I_t(x,y,t) = I_o(x,y) + I_r(x,y) + 2A_o(x,y)A_r(x,y)\cos\left[\Delta f(x,y) + W_t(x,y,t)\right] . \tag{11}$$

Since the CCD camera registers average intensity at the video rate characterized by the period Δt which, in the EOH system used in this study is equal to 1/30-th of a second, the intensity that is observed can be expressed mathematically as

$$I(x,y) = \frac{1}{\Delta t}\int_{t}^{t+\Delta t} I_t(x,y,t)\,dt , \tag{12}$$

and, using phase stepping, the resultant intensity distribution for the n-th frame can be written as

$$I_n(x,y) = I_o(x,y) + I_r(x,y) + 2A_o(x,y)A_r(x,y)\cos\left[\Delta f(x,y) + \Delta q_n\right] M\left[W_t(x,y)\right] , \tag{13}$$

where $M\left[W_t(x,y)\right]$ is known as the characteristic function determined by the temporal motion of the object. For the case of sinusoidal vibrations with the period much shorter than the video framing time

$$M\left[W_t(x,y)\right] = J_o\left[W_t(x,y)\right] , \tag{14}$$

where $J_o\left[W_t(x,y)\right]$ is the zero order Bessel function of the first kind[3]. Equation 13 contains four unknowns: irradiances I_o and I_r, phase difference Δf, and the fringe-locus function W_t. The EOH's video frame processing algorithm eliminates Δf from the argument of the irradiance function given by Eq. 13, using a set of four equations obtained at specific step size value Δq.

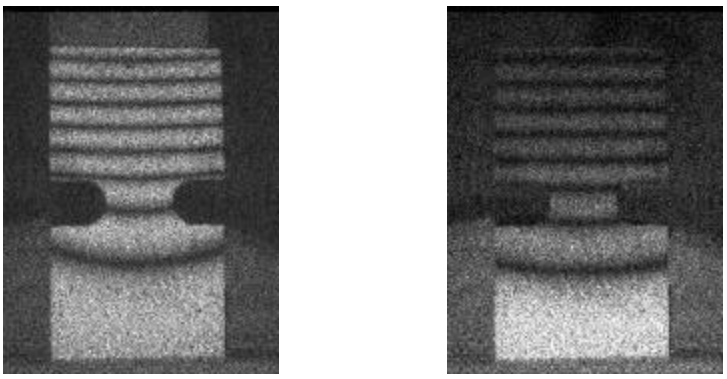

(a) (b)

Fig. 3. Typical interferograms obtained using the EOH: (a) static mode (double-exposure), (b) dynamic mode (time-average exposure).

For time-average investigations, the EOH can work in display and data modes. In the display mode, interference patterns are observed at video rate and are modulated by a function of the form

$$4A_o A_r \left| M(W_t) \right| \quad , \tag{15}$$

this mode is used for adjusting the EOH system and for qualitative investigations. Figure 3b shows a typical interferogram of a sinusoidally excited plate, as recorded by the EOH system functioning in the time-average display mode. The data mode is used for performing quantitative investigations[3,4,10]. In the data mode, images of the form

$$16 I_o I_r M^2(W_t) \quad , \tag{16}$$

are generated for quantitative processing and extraction of W_t.

2.2.3. Shape measurements using EOH

With the EOH, it is possible to perform noninvasive static and dynamic investigations of mechanical components subjected to a large variety of loading conditions[3]. In addition, it is also possible to measure shape of mechanical components using optical contouring[11]. The combination of these capabilities makes the EOH a powerful engineering tool that can be utilized for the study and optimization of mechanical components. Recent technological advances in computer and fiber optic technologies can be applied to the EOH system. These advances dramatically increase the versatility of the EOH method and add the possibility of using it in on-site investigations in order to study and diagnose problems in industrial environments.

Figure 4 depicts a currently operational EOH system used for static, dynamic, and shape measurement investigations. This system is based on a single illumination and single observation directions. The light source is a low power laser diode LD with thermo-electric cooling capabilities driven by the controller LDD which provides the laser diode with the adequate current for generation of light emission and temperature control. The output of the laser diode is directed through a Faraday optical isolator OI, which reduces the magnitude of back reflected light into the LD, to a microscope objective MO coupling it into a single mode fiber optic directional coupler DC. This directional coupler splits the light power into a 1:9 ratio. The higher power beam is used for illumination of the object of interest and the lower power beam is used as a reference beam. Both beams are recombined in the interferometer SI and the acquired irradiances transmitted to an image processing computer IP through the use of a CCD camera. PZT_1 is a piezo-electric fiber optic modulator for phase stepping, and PZT_2 is similar to PZT_1 but used for introduction of a bias signal for quantitative analysis of time-average interferograms. This setup occupies a minimum space and can be readily rearranged to obtain different experimental configurations.

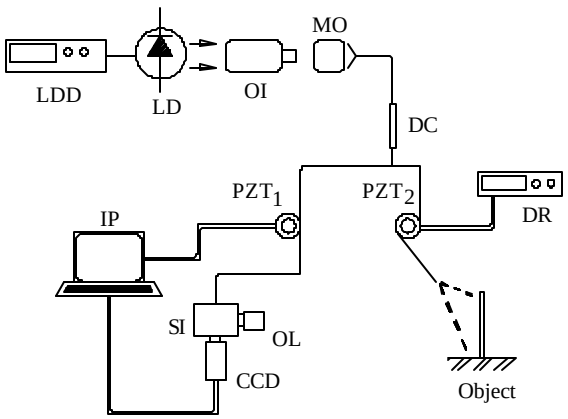

Fig. 4. Single illumination, single observation fiber optic based EOH system: LDD is the laser diode driver, LD is the laser diode, OI is the optical isolator, MO is the microscope objective, DC is the directional coupler, PZT_1 and PZT_2 are the piezo-electric fiber optic modulators, DR is the PZT_2 driver, IP it the image processing computer, SI is the interferometer, OL is the objective lens, and CCD is the camera.

The EOH system shown in Fig. 4 uses the two-wavelength technique for generation of depth contours related to the geometry of the object under investigation. The wavelength of the laser diode used can be controlled either by modulating its injection current or by modifying the temperature of the thermally controlled stage of the diode. Contouring can be performed by using the EOH in static mode. This is done by acquiring a set of interferograms using wavelength λ_1 representing a reference state, or undeformed state, and then acquiring the second set of interferograms after wavelength has been changed to λ_2 representing a modified state, or deformed state. The phase change related to depth contours $g(x,y)$ obtained after performing this operation is now equivalent to the fringe-locus function $W(x,y)$ in static deformations, so Eqs 6 to 10 hold for $g(x,y)$. Figure 5 depicts some typical results obtained after contouring a 3D mechanical component: a jet engine turbine blade. For this particular application, collimated retro-reflective conditions were utilized in order to obtain the fringe separation of

$$h = \frac{\lambda_{12}}{2} \quad , \tag{17}$$

where $\lambda_{12} = \lambda_1 \lambda_2 / |\lambda_1 - \lambda_2|$.

2.3. Fringe prediction

Fringe prediction (FP) is an important part of the hybrid, experimental and computational, approach presented in this paper. FP is used for interacting between information provided by FE and EOH investigations. This interaction can provide valuable information that can be utilized for increasing the degree of correlation between the computational and the experimental results.

FP can be used to specify the appropriate parameters for performing successful EOH investigations before making the actual measurements. This is of particular importance, specially for complicated mechanical components, since the magnitude and location of the experimentally applied loads is not easy to determine. The objective of FP, in this case, is to specify loading conditions such that at areas of interest on the object, phase change can be measured accurately. This means that phase changes must be large with respect to the sensitivity of the EOH system and small enough to prevent speckle decorrelation from ruining the measurements, since there is requirement of a minimum number of pixels per fringe needed for successful phase unwrapping. Figures 6 to 8 show representative applications of the FP.

Figure 6 shows an AL-2024 plate of 15x15 mm and 110 μm thick constrained along all four edges vibrating at its first fundamental mode. This figure depicts overloaded (Fig. 6a) and appropriate loading (Fig. 6b) condition levels for quantitative EOH investigations.

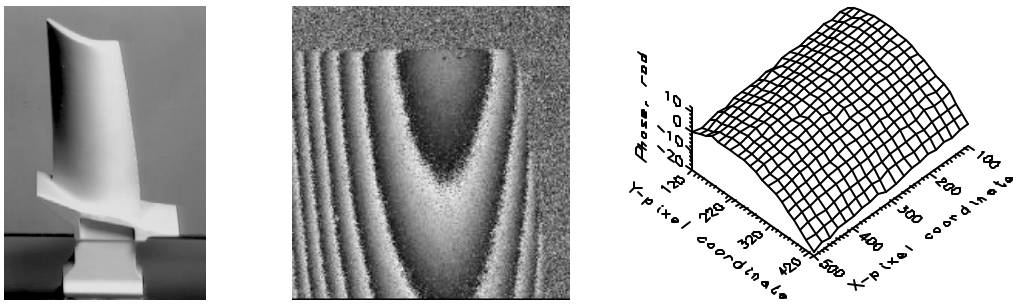

(a) (b) (c)

Fig. 5. Contouring the tip of a turbine blade with $\Delta l \approx 0.1$nm: (a) object as used in the experimental setup, (b) wrapped phase in the area of interest, (c) wireframe representation of the unwrapped phase in the area of interest.

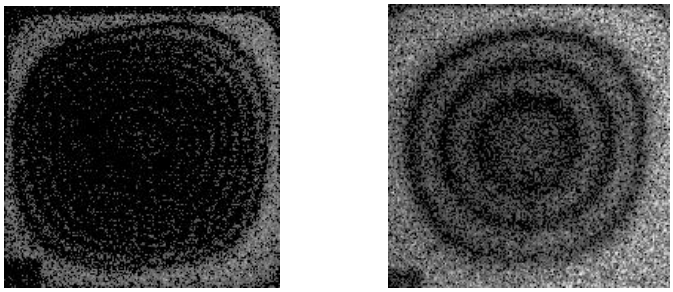

(a) (b)

Fig. 6. Interferograms showing: (a) specimen overloaded - difficult to perform quantitative interpretation (b) specimen loaded at an appropriate level - quantitative interpretation can be readily performed.

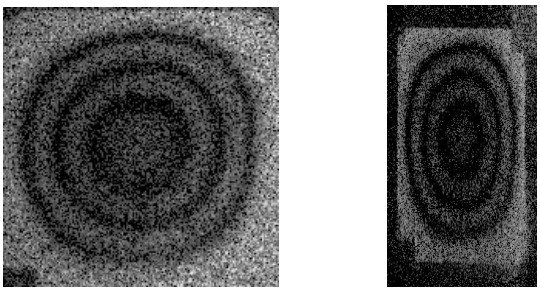

(a) (b)

Fig. 7. Interferograms showing the effects of different sensitivity vectors: (a) retro-reflective illumination/observation condition, (b) oblique illumination/observation condition.

FP can also be utilized for simulation of different experimental arrangements characterized by the sensitivity vector $\boldsymbol{K}$, see Eq. 5, and, in this way, lead to optimization of the setup in order to facilitate specific applications of the EOH. In addition, FP is useful for effective comparison of experimental and computational results because it takes into consideration the actual experimental illumination/observation conditions while interpreting (displaying) computational data. Figure 7 shows typical interferograms of a component loaded under similar conditions, but using two experimental setups with different sensitivity vectors, and demonstrates the importance of taking into consideration the illumination/observation conditions when performing comparisons between experimental and computational results.

FP can be performed by:

(a) theoretical/computational modeling using theoretically/experimentally obtained boundary conditions and/or loads, theoretically/experimentally obtained geometry, and experimentally obtained material properties,

(b) use of computational nodal information at the object boundary,
(c) orientation of theoretical/computational geometry to match experimental conditions,
(d) evaluation of the fringe-locus function W, or evaluation of the time varying fringe-locus function W_t,
(e) use of the *cosine* or J_o irradiance distributions while considering optical configuration of the specific EOH setup in which characteristics of optical components affecting laser beam profile (e. g., Gaussian) are taken into consideration.

Figure 8 depicts FP on a cantilever beam loaded under static bending conditions.

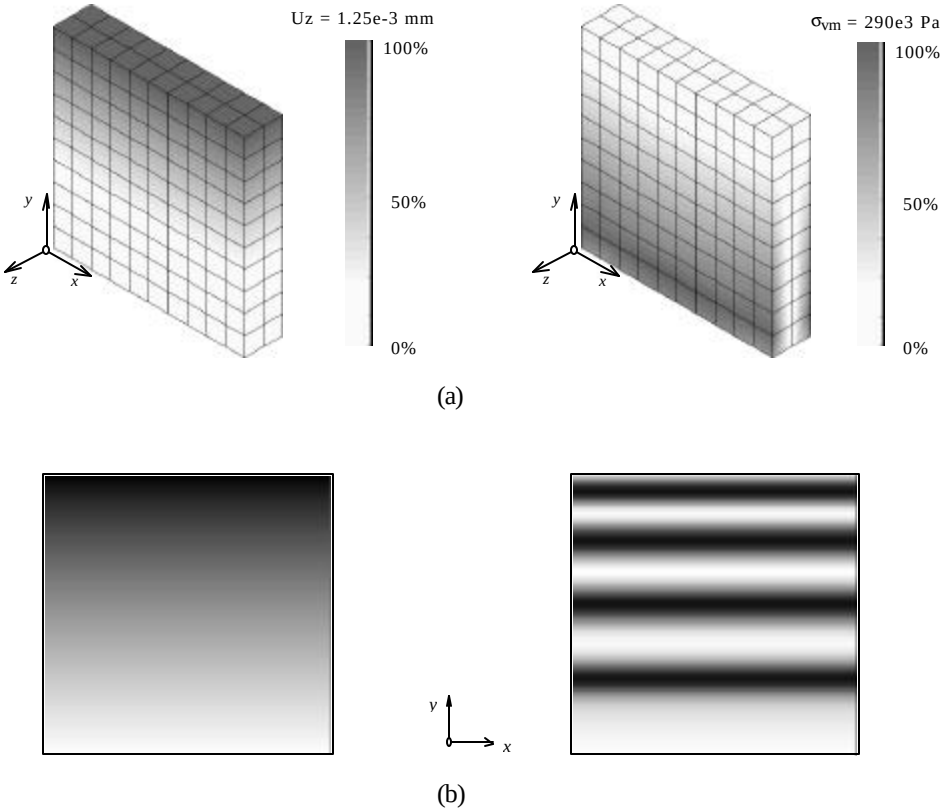

Fig. 8. Fringe prediction based on computational simulations of a cantilever beam loaded under static bending conditions: (a) finite element solutions for displacement and stress, (b) predicted continuous (unwrapped) phase map corresponding to a double-exposure hologram assuming collimated retro-reflective illumination/observation conditions and the resulting fringe pattern.

2.3.1. Use of EOH-FEM-FP as a hybrid experimental - computational tool

Computational techniques are capable of predicting surface and interior displacements of an object of interest subjected to specific loading and boundary conditions. With these techniques, it is possible to perform parametric investigations[7]. However, computational investigations are only reliable if proper geometry, boundary conditions, loadings, and material properties are provided. Unexpected defects on the object of interest may cause computational simulations to deviate from the actual behavior of the object.

For the description of the actual geometry of an object under investigation, shape measurements using the EOH may be useful. In addition, qualitative and quantitative information obtained in static and dynamic EOH modes can be utilized as boundary conditions in a computational model. Also, a computational model can be used for prediction of interferometric fringes which can be useful for determination of appropriate experimental parameters and setup as well as a tool for verifying that realistic boundary conditions have been applied accurately.

Figure 9 depicts the interaction of EOH, FEM, and FP in hybrid experimental - computational investigations. Quantitative and qualitative results provided by the EOH methodology are utilized by or compared with the FE predictions[4]. FP is used as a complementary step for measuring the degree of correlation between EOH and FE results and to provide feedback to either method in order to improve the results of the hybrid analysis.

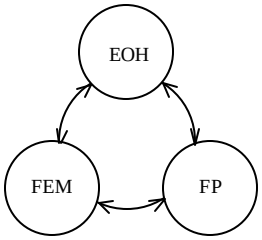

Fig. 9. Interaction of EOH, FEM, and FP in the hybrid, experimental and computational, investigations.

2.4. Hybrid, experimental and computational, procedure

Figure 10 depicts a flowchart of the hybrid, experimental-computational, procedure used in this paper[7]. According to Fig. 10 computational investigations are performed on the initial design in order to obtain the response of the structure before its structural optimization is performed and the results compared with the response obtained from the EOH studies of an equivalent initial design model. The comparisons between experimental and computational results are based on FP. When discrepancies between computational and experimental results are encountered it is necessary to resolve them. These authors have found that one of the most effective ways to achieve such a resolution is by the use of experimentally obtained boundary conditions in the computational model. Verifications also include characterization of material constants, geometric modeling accuracy, and mechanical and optical setups. The results of these comparisons provide information on the accuracy of the computational analyses with respect to modeling the experimental behavior of the structure. When an acceptable degree of accuracy is obtained the computational model is applied to perform sensitivity analyses of the objective function with respect to the specified design variables as well as shape optimization of the initial design. The geometry obtained from the shape optimization analyses is used to manufacture a prototype which is experimentally tested in order to obtain computational and experimental comparisons through the FP operation.

3. REPRESENTATIVE APPLICATION OF THE HYBRID, EXPERIMENTAL AND COMPUTATIONAL, APPROACH

The hybrid approach was applied to the study of the fundamental mode of vibration of an Al-2024 plate, 15x15 mm and 110 μm thick constrained at the edges. Analysis was performed using classical plate theory and modeled with a commercially available FE package: COSMOS/M. The FE model used 256 thin shell elements with six degrees of freedom per node. Since it was expected to obtain a mode shape with a maximum displacement at the center of the plate, higher element density was used at this location. Perfect zero displacements applied at the edges of the plate were used as boundary conditions and elastic material constants were obtained from experimental data[12]. The fundamental mode of vibration was obtained after solving the corresponding characteristic eigenvalue problem with the inverse power iteration method. This yielded a natural frequency of 6.92 kHz. Figure 11a depicts the corresponding mode shape.

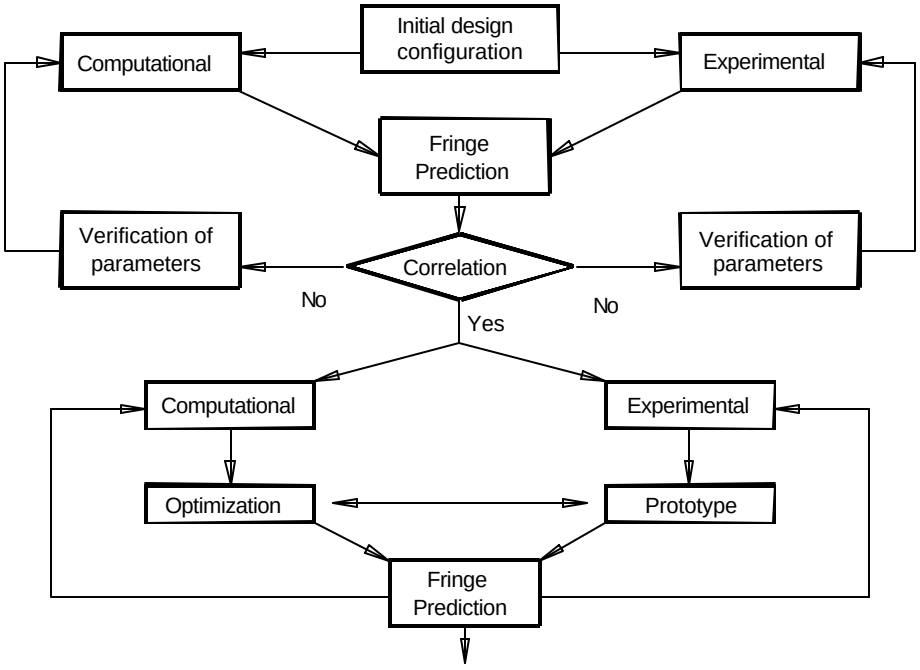

Fig. 10. Flowchart of the hybrid, experimental and computational, procedure used in this paper.

Experimental modal analysis was performed using the EOH system in the time-average mode. The sample was mounted on a special fixture and excited with a piezo-electric shaker which in turn was driven by a frequency generator. The EOH system displayed time-average interferograms at video speed when the excitation frequency was modulated. This procedure allowed the determination of the fundamental natural frequency and mode shape of interest. Figure 11b depicts the observed fundamental mode of the plate obtained at 6.52 kHz. Collimated retro-reflective conditions were held.

Using displacement information obtained from theoretical and computational results, FP was performed using collimated retro-reflective conditions. Figure 12 depicts predicted double-exposure and time-average interferograms. Comparisons between observed and predicted interferograms show mode shape discrepancies. In addition, theoretical solutions show that the mode shape $w(x,y)$ should have the form

$$w(x,y) = \left(\cos\frac{2\pi x}{a} - 1\right)\left(\cos\frac{2\pi y}{b} - 1\right) , \tag{18}$$

where a and b are the plate dimensions and $x \in [0,a]$ and $y \in [0,b]$. Equation 18 predicts a symmetrical mode shape which is not observed experimentally, therefore, attention was concentrated on the experimental investigations. In addition, Eq. 18 indicates that mode shape depends on the plate dimensions as well as on correct application of boundary conditions, i. e., zero displacements at all of the edges. With this observation, as well as information provided by the FP of time-average interferograms, Fig. 12b, experimental boundary conditions were verified. Results of these verifications provided a new observed mode shape, Fig. 13, and a resonance frequency of 7.06 kHz. The result shown in Fig. 13 should be compared with that shown in Fig. 11b to realize differences between the mode shape based on the hybrid approach versus that without the experimental verification/validation, respectively.

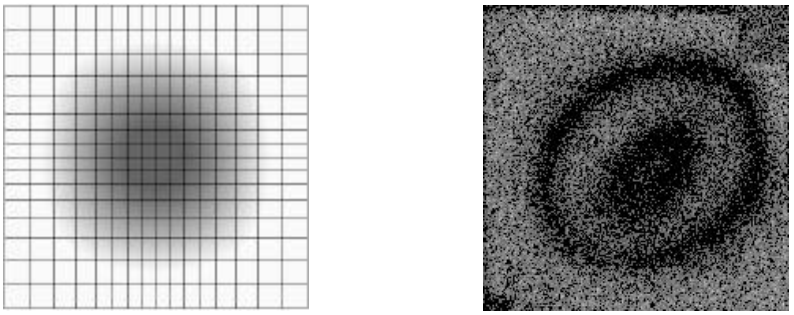

(a) (b)

Fig. 11. Typical results obtained without using the hybrid experimental-computational approach: (a) analytical/computational solution, (b) time-average interferogram.

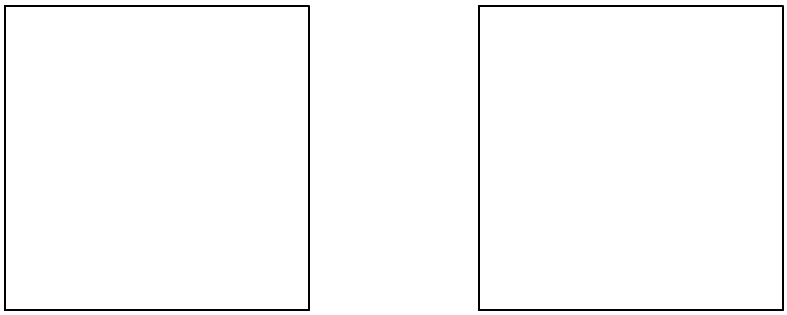

(a) (b)

Fig. 12. Predicted fringe patterns based on analytical/computational solutions: (a) static (double-exposure), and (b) dynamic (time-average).

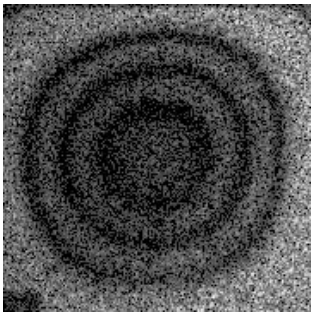

Fig. 13. Interferogram obtained after verification of the boundary conditions.

4. CONCLUSIONS AND RECOMMENDATIONS

Computational techniques are very powerful methods for analysis of structural components and parametric investigations for determination of critical conditions. However, these techniques may lack any significance if incorrect input parameters, e. g., boundary conditions, loads, and material properties, are utilized. Experimental studies using electro-optic techniques have the characteristic of being

able to obtain noninvasive measurements of the actual behavior of mechanical components subjected to specific loads and boundary conditions. In this study, computational investigations, electro-optic holography, and fringe prediction was discussed as a hybrid approach for an effective study and structural optimization of mechanical components. Practical application of the hybrid approach is illustrated by a representative example, which demonstrates viability of this approach as an engineering tool for structural analysis and optimization.

5. ACKNOWLEDGMENTS

This study was supported by the Flight Dynamics Directorate, Wright Laboratory, Aeronautical Systems Division (AFSC), United States Air Force, Wright-Patterson AFB, OH 45433-6553. The authors would also like to thank all members of the CHSLT for their helpful discussions and assistance during preparation of this paper.

6. REFERENCES

1. Pro/MECHANICA user's guide v. 16, Parametric Technology Corporation, Waltham, MA, 1996.

2. T. Haftka and R. V. Grandhi, "Structural shape optimization-a survey," *Comp. Meth. in App. Mech. and Eng.*, 57:91-106, 1986.

3. R. J. Pryputniewicz, "Quantitative determination of displacements and strains from holograms," Ch. 3 in P. K. Rastogi, ed., *Holographic interferometry*, Springer-Verlag, Berlin, pp. 33-72, 1994.

4. R. J. Pryputniewicz and K. A. Stetson, "Measurement of vibration patterns using electro-optic holography," *Proc. SPIE*, 1162:456-467, 1989.

5. COSMOS/M user's guide v. 1.70, Structural Research and Analysis Corporation, Santa Monica, CA, 1993.

6. O. C. Zienkiewicz and R. L. Taylor, *The finite element method: solid and fluid mechanics, dynamics, and nonlinearities*, Vol. 2, McGraw-Hill, New York, 1991.

7. C. Furlong and R. J. Pryputniewicz, "Opto-mechanical study and optimization of a cantilever plate dynamics," *Proc. SPIE*, 2545:192-203, 1995.

8. C. Furlong and R. J. Pryputniewicz, "New opto-mechanical approach to quantitative characterization of fatigue behavior of dynamically loaded structures," *Proc. SPIE*, 2544:45-56, 1995.

9. B. E. A. Saleh and M. C. Teich, *Fundamentals of photonics*, Wiley, New York, 1991.

10. T. W. Bushman, *Automated fringe unwrapping by energy minimization*, MS Thesis, Worcester Polytechnic Institute, Worcester, MA, 1993.

11. C. M. Vest, *Holographic interferometry*, Wiley, New York, 1979.

12. C. Furlong and R. J. Pryputniewicz, "Study of the elastic-plastic behavior of the spherical nanoindentation process," *Proceedings of the 1995 SEM Spring Conference*, 1:727-734, Grand Rapids, MI, 1995.
